

THE INFRARED SPECTRAL ENERGY DISTRIBUTION OF THE SEYFERT 2 PROTOTYPE NGC 5252

M. ALMUDENA PRIETO

European Southern Observatory, D-85748 Garching, Germany; and Instituto de Astrofísica de Canarias, La Laguna, Spain; aprieto@eso.org

AND

J. A. ACOSTA-PULIDO

Instituto de Astrofísica de Canarias, La Laguna, Spain; jap@ll.iac.es

Received 2002 January 7; accepted 2002 October 4

ABSTRACT

The complete mid- to far-infrared continuum energy distribution collected with the *Infrared Space Observatory* of the Seyfert 2 prototype NGC 5252 is presented. ISOCAM images taken in the 3–15 μm show a resolved central source that is consistent at all bands with a region of about 1.3 kpc in size. Because of the lack of ongoing star formation in the disk of the galaxy, this resolved emission is associated with either dust heated in the nuclear active region or bremsstrahlung emission from the nuclear and extended ionized gas. The size of the mid-IR emission contrasts with the standard unification scenario envisaging a compact dusty structure surrounding and hiding the active nucleus and the broad-line region. The mid-IR data are complemented by ISOPHOT aperture photometry in the 25–200 μm range. The overall IR spectral energy distribution is dominated by a well-defined component peaking at $\sim 100 \mu\text{m}$, a characteristic temperature of $T \simeq 20 \text{ K}$, and an associated dust mass of $2.5 \times 10^7 M_{\odot}$, which greatly dominates the total dust mass content of the galaxy. The heating mechanism of this dust is probably the interstellar radiation field. After the contribution of this cold dust component is subtracted, the bulk of the residual emission is attributed to dust heated within the nuclear environment. Its luminosity consistently accounts for the reprocessing of the X-ray to UV emission derived for the nucleus of this galaxy. The comparison of NGC 5252’s spectral energy distribution with current torus models favors large nuclear disk structure on the kiloparsec scale.

Subject headings: galaxies: active — galaxies: individual (NGC 5252) — galaxies: photometry — galaxies: Seyfert — infrared: galaxies

1. INTRODUCTION

NGC 5252 is one of the best examples of anisotropy of the nuclear radiation field. It exhibits a perfect biconical morphology of extranuclear ionized gas (Tadhunter & Tsvetanov 1989), extending out to $\sim 45''$ – $50''$, equivalent to $\sim 20 \text{ kpc}$,¹ and neutral H I gas filling the regions outside the bicone of ionized gas (Prieto & Freudling 1993). Such selective distribution of gas implies an intrinsically collimated radiation field at least at the extended narrow-line region scale.

NGC 5252 has been subjected to a wide range of multi-wavelength observations from the X-ray to the radio domain. A large fraction of the observations were aimed at revealing the nature and geometry of the postulated obscuring material responsible for blocking the nuclear light in directions outside the bicone of ionized gas. The observational evidence points to a heavily obscured nucleus and the broad-line region: a band of red material lying across the nucleus and perpendicular to the bicone of ionized gas is seen in near-IR–optical ratio maps of the galaxy (Kotilainen & Prieto 1995). The presence of an obscured nucleus is also confirmed in the high-energy domain. The 0.4–10 keV *ASCA* spectrum of the galaxy (Cappi et al. 1996) reveals a heavily obscured nucleus with $N(\text{H}) \sim 4.3 \times 10^{22} \text{ cm}^{-2}$. This implies about 20 mag of extinction in the visible, sufficient to absorb all the nuclear optical and UV light in the line of sight. On the other hand, broad permitted lines have been observed in the optical (Acosta-Pulido et al. 1996;

Osterbrock & Martel 1993) and near-IR (NIR) range (Ruiz, Rieke, & Schmidt 1994; Goodrich, Veilleux, & Hill 1994). The modeling of the nuclear spectral energy distribution (SED) and line spectrum in NGC 5252 is consistent with the nuclear ionizing radiation being heavily absorbed (Contini, Prieto, & Viegas 1998).

Because of the heavy central obscuration advocated by the above observations, the mid- to far-IR region becomes an ideal window for studying the nuclear emission in detail. The 20 mag extinction measured in the optical reduces to about 1.5 mag at 10 μm . This paper presents new photometric data covering the mid- to far-IR range (from 3 to 200 μm). Together with NIR data available from the literature, one of the most complete IR SEDs among Seyfert galaxies is presented. In contrast to most Seyfert galaxies, NGC 5252 shows no evidence for star formation activity across its disk: H α imaging reveals the distribution of ionized gas to be restricted to the nucleus and the bicone only (Prieto & Freudling 1996; Tsvetanov, Morse, & Cecil 1996). This unique advantage makes of NGC 5252 an ideal target for pursuing “clean” studies of its central nuclear emission.

2. THE DATA

Mid-IR images of NGC 5252 were obtained in several filters using the ISOCAM instrument (Cesarsky et al. 1996) on board the *Infrared Space Observatory* (ISO).² A total of

¹ NGC 5252 has a redshift $z \simeq 0.0230$, which gives a scale of $\simeq 433 \text{ pc arcsec}^{-1}$, adopting $H_0 = 75 \text{ km s}^{-1} \text{ Mpc}^{-1}$.

² Based on observations with *ISO*, an ESA project with instruments funded by ESA member states (especially the PI countries, France, Germany, the Netherlands, and the United Kingdom) and with the participation of ISAS and NASA.

TABLE 1
NUCLEAR PHOTOMETRY OF NGC 5252

Filter	λ (μm)	Aperture (arcsec)	F_ν (mJy)	Reference
5230 Å.....	0.52	3	1.1	1
	0.52	Nuclear	0.012	1
7027 Å.....	0.70	3	2.7	1
	0.70	Nuclear	0.053	1
<i>J</i>	1.25	3	11.0	1
	1.25	Nuclear	11.0	1
<i>H</i>	1.65	3	15.0	1
	1.65	Nuclear	2.6	1
<i>K</i>	2.2	3	13.0	1
	2.2	Nuclear	3.78	1
CAM-SW6.....	3.72	15	16.6	2
CAM-LW5.....	6.75	15	20 \pm 5	2
CAM-LW7.....	9.63	15	34 \pm 6	2
CAM-LW8.....	11.37	15	48 \pm 6	2
IRAS-12.....	12	15	40:	3
CAM-LW3.....	14.5	15	47 \pm 7	2
CAM-LW9.....	15	15	63 \pm 8	2
PHT-P25.....	25	60	75.0 \pm 60	2
IRAS-25.....	25	...	56:	3
IRAS-60.....	60	90	425 \pm 55	3
PHT-C60.....	60	60	380 \pm 110	2
PHT-C90.....	90	70	498 \pm 150	2
IRAS-100.....	100	90	750 \pm 130	3
PHT-C120.....	120	...	840 \pm 70	2
PHT-C135.....	150	...	1060 \pm 50	2
PHT-C180.....	180	...	710 \pm 50	2
PHT-C200.....	200	...	570 \pm 160	2
CO(2-1).....	1332	...	27:	4
CO(1-0).....	2677	...	21:	4

NOTE.—Colons indicate an upper limit.

REFERENCES.—(1) Kotilainen & Prieto 1995; (2) this article; (3) Edelson et al. 1987; (4) Prieto & Freudling 1996.

eight filters were used (see Table 1): five centered on the continuum at 15, 14.5, 11.37, 6.75, and 3.72 μm , respectively, and three in the polycyclic aromatic hydrocarbon (PAH) emission at 3.3 μm , CO line at 4.7 μm , and the broad Si absorption feature at 9.63 μm , respectively. The pixel field of view was 3". All images were collected following a micro-scanning pattern of 3 \times 3 points and a step size of 2" in both x - and y -directions. In this way the point-spread function (PSF) was oversampled, which allows a better detection of possible extended emission. The data were processed using version 4.0 of CIA (Ott et al. 1997). This was used for dark signal subtraction, deglitching, drift correction (for the LW camera) using the Fouks & Schubert (1995) formula, flat-fielding, flux calibration, and mosaicking. Unfortunately, the images in the 3.3 and 4.7 μm filters (taken with the SW camera) are affected by hysteresis that could not be corrected.

Integrated aperture photometry in the 25–200 μm range measured by ISOPHOT (Lemke et al. 1996) are also presented. The ISOPHOT data were reduced using PIA version 9.1 (Gabriel et al. 1997) following the standard signal corrections (Laureijs et al. 2000, *ISO Handbook*)³ except for signal nonlinearity, which was not applied. The observation in chopped mode at 25 μm was calibrated by using a mean

value of detector responsivity corrected for systematic variation with orbital position (Abraham et al. 2003). In the other cases, the internal calibrators were used to determine the responsivity. Because of the faintness of the source, the fluxes at 60 and 90 μm were derived using only the central pixel of the ISOPHOT-C100 array, after correction for signal losses due to partial covering of the PSF. These values were recalibrated by the scaling factors 0.8 and 1.27 at 60 and 90 μm , respectively. These scaling factors were derived after comparison of the fluxes as measured by ISOPHOT at those bands and measured by *IRAS* at 60 and 100 μm of a sample of CfA Seyfert galaxies (González-Hernández et al. 2003, in preparation). The *IRAS* data at 60 and 100 μm (Edelson, Malkan, & Rieke 1987) were also included in the analysis. The fluxes measured at filters beyond 120 μm were recalibrated after comparison of the background measurements with respect to the corresponding values in the *COBE*/DIRBE maps.

3. RESULTS

3.1. Extended Mid-IR Emission

The IR emission of NGC 5252 in the ISOCAM images (3–15 μm range) is concentrated to the nuclear region, yet the emission is marginally extended in all the filters. The extended nature of the emission was assessed in the two following ways. First, each image was compared with the modeled ISOCAM point-spread function (PSF) corresponding to each filter (K. Okumura 1998, ISOCAM PSF Report).⁴ In all cases, the galaxy profile was found broader than the theoretical PSF. Second, a comparison with a measurement of a calibration star observed with exactly the same raster configuration as that used for NGC 5252 was used. This comparison could only be done at 15 μm (LW3 filter) because no other stars with the same observation configuration exist in the *ISO* archive (Fig. 1). This comparison was

⁴ The ISOCAM PSF report is available at http://www.iso.vilspa.esa.es/users/exp1_lib/CAM_list.html.

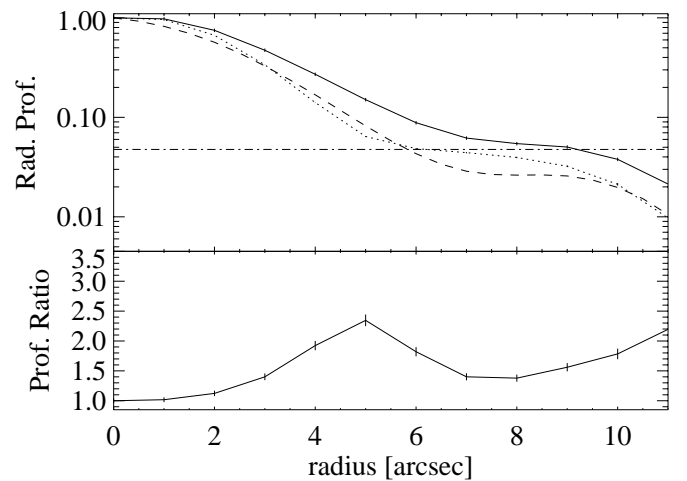


FIG. 1.—Normalized radial intensity profiles of NGC 5252 at 15 μm (solid line). For comparison, the theoretical (dashed line) and the observed (dotted line) PSFs are also shown. The horizontal line represents the detection limit as measured by the 3 σ of the image background. The ratio between the NGC 5252 radial profile and the observed PSF is represented in the bottom panel. The difference between the theoretical and the observed PSFs at the inner radii is due to the pixel sampling.

³ The *ISO Handbook*, Volume V, is available at http://www.iso.vilspa.esa.es/manuals/HANDBOOK/V/pht_hb.

conclusive. The measured FWHM of the galaxy profile at $15\ \mu\text{m}$ is $5''.6$, whereas that of the stellar profile is $4''.6$ (Fig. 1). After deconvolving for the PSF width, an extension of $\approx 3''.3$ consistent in all filters is found.⁵ The compactness of the emission in the ISOCAM images hampers however any morphology definition.

Previous claims regarding the presence of obscuring structure in the circumnuclear region of this galaxy are reported by Kotilainen & Prieto (1995): a redder nuclear band, perpendicular to the ionized gas bicone and extending $\sim 5''$ east-west across the nucleus was found in near-IR optical color maps. Tsvetanov et al. (1996), on the basis of *Hubble Space Telescope* optical observations, reported on a D-shaped obscuring structure northeast of the nucleus with a size of $\sim 3''$. Thus, although the morphology of the mid-IR emission is undetermined, its size is consistent with that of the reported obscuring nuclear structures seen in the near-IR and optical images.

There are few Seyfert galaxies in which the mid-IR emission is known to be extended. In NGC 1068, the emission from 7.9 to $25\ \mu\text{m}$ extends over a few arcseconds, aligning with the radio jet and roughly correlating with the [O III] morphology (Cameron et al. 1993; Bock et al. 2000). Bock et al. (2000) found that about $\frac{2}{3}$ of the total emission is contained in an unresolved central core ($0''.1$ resolution) and the other $\frac{1}{3}$ in the extended emission. Krabbe, Böker, & Maiolino (2001) report on the detection of extended mid-IR emission in Circinus and NGC 3281.

3.2. IR Spectral Energy Distribution

The IR spectral energy distribution of NGC 5252 including the new ISOCAM and ISOPHOT data is shown in Figure 2. The stellar-subtracted nuclear continuum fluxes in the near-IR to optical range by Kotilainen & Prieto (1995) are also shown. A clear feature in the SED is the prominent bump enclosing the 60 – $200\ \mu\text{m}$ range and dominating the continuum emission.

Up to *IRAS*, the bulk of IR emission in active galaxies has in general been associated with dust reprocessing of the intense UV–optical nuclear radiation. Although still lacking spatial resolution, the wider wavelength coverage and better sampling of the IR continuum by *ISO* has allowed Pérez García & Rodríguez Espinosa (2001) to discern three main IR components in the SED of Seyfert galaxies. These are a very cold component ($T \sim 15$ – 20 K), corresponding to dust heated by the interstellar radiation field; a cold component ($T \sim 40$ – 50 K), which is associated with star-forming regions; and a warm component ($T \sim 100$ – 200 K) associated with dust heated by the active nucleus and/or nuclear starbursts. As our IR wavelength coverage for NGC 5252 gets up to the near-IR, a simple parameterization of its SED as the sum of a minimum number of modified blackbodies was introduced. This parameterization has the purpose of getting a characteristic value of the luminosity, temperature, and mass of the typical dust. Figure 2 shows the fit to the SED as the sum of a minimum five modified blackbodies

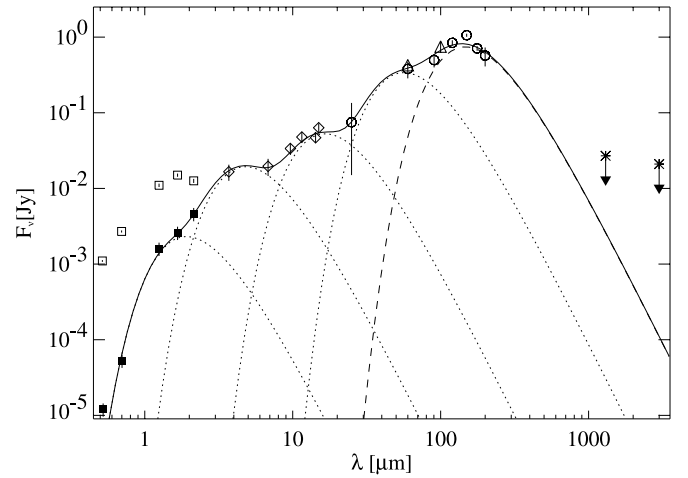


FIG. 2.—IR spectral energy distribution of NGC 5252. Circles represent ISOPHOT photometric data; diamonds, ISOCAM data; triangles, *IRAS* data. For the sake of clarity, *IRAS* upper limits at 12 and $25\ \mu\text{m}$ are not included. The open and filled squares represent the $3''$ aperture and stellar-subtracted nuclear fluxes, respectively, from Kotilainen & Prieto (1995). Two upper limits in the submillimetric range are included (Prieto & Freudling 1996). The continuous line is a parameterization of the SED as the sum of five modified blackbodies with $T = 20, 50, 175, 600$, and 1500 K. The coolest component is represented by the dashed line and the other blackbody components as dotted lines. The SED shows its maximum at $\sim 100\ \mu\text{m}$.

with $T = 20, 50, 175, 600$, and 1500 K.⁶ It should be stressed that regardless of this parameterization, the local bump at 90 – $200\ \mu\text{m}$ is by itself well defined by a single modified blackbody with $T \sim 20$ K. We will single out this component as a different one from the rest of the IR SED. The arguments are as follows.

Danese et al. (1992) showed that most of the far-IR (*IRAS* at 60 and $100\ \mu\text{m}$) emission in Seyfert galaxies is unrelated to nuclear activity. Pérez García & Rodríguez Espinosa (2001) and Acosta-Pulido et al. (2001) reached the same conclusion on the basis of a much wider and better sampled spectral energy range covered by the 16 – $200\ \mu\text{m}$ ISOPHOT data. Recently, Prieto, Pérez García, & Rodríguez Espinosa (2001, 2002) showed that the X-ray emission and the coronal line emission in Seyfert galaxies, both being typical indicators of the nuclear activity, are correlated with the mid-IR emission but unrelated to the far-IR emission. In the case of NGC 5252, the lack of star formation in the disk of the galaxy (§ 1), the absence of dust lanes or knots across its disk, as evidenced in optical–IR color maps (Kotilainen & Prieto 1995), and the compactness of the emission in the 3 – $15\ \mu\text{m}$ range lead us to argue that the bulk of the near- to mid-IR emission is of nuclear origin, whereas the far-IR emission, represented by the 20 K component, is a separate component, unrelated to the nuclear activity. This component is associated with the galaxy as a whole and is most probably due to dust heated uniformly across the galaxy by the interstellar radiation field.

⁵ There are slight discrepancies between the theoretical PSF and that of the star profile that affect the peak of the function and the wings (see discussion by K. Okumura 1998). However, the difference between the FWHMs of both PSFs never exceeds 10% for the filters used here.

⁶ We have also tried the inversion method described by Pérez García, Rodríguez Espinosa, & Santolaya Rey (1998). Their method yields seven components with temperatures $T = 20, 50, 133, 182, 380, 820$, and 1500 K. The differences between our decomposition and theirs appear at the gaps in the SED (2 – 7 and 25 – $60\ \mu\text{m}$); however, the main components at 20 and 50 K are preserved.

TABLE 2
DERIVED IR PROPERTIES OF NGC 5252

Component	Temperature (K)	F_{IR} (ergs cm ⁻² s ⁻¹)	L_{IR} (ergs s ⁻¹)	M_{dust} (M_{\odot})
Galaxy	20 ± 4	$(1.7 \pm 0.5) \times 10^{-11}$	$(1.8 \pm 0.5) \times 10^{43}$	$(2.5 \pm 1.0) \times 10^7$
Nuclear	50–1500	$(5.0 \pm 0.8) \times 10^{-11}$	$(5.3 \pm 0.8) \times 10^{43}$	1.0×10^5
Total	$(6.2) \times 10^{-11}$	$(6.5) \times 10^{43}$	$(2.5 \pm 1.0) \times 10^7$

The luminosity, temperature, and dust mass associated with the galaxy component (20 K) and with the nuclear component (sum of the other blackbodies) was estimated following Kennicutt (1998) and is provided in Table 2.

4. DISCUSSION

4.1. Origin of the Extended Mid-IR Emission

The size of the extended mid-IR emission detected in NGC 5252 corresponds to an emitting region of ~ 1.3 kpc.

According to the previous SED decomposition, dust emitting at the mid-IR waves should reach temperatures $\simeq 175$ K (see also Pérez García & Rodríguez Espinosa 2001). The luminosity associated with this warm component is 1.1×10^{-11} ergs cm⁻² s⁻¹. Most of this emission should come from the nucleus but not necessarily all. For example, in NGC 1068, $\frac{1}{3}$ of the $10 \mu\text{m}$ emission is extended across the nucleus. Some plausible mechanisms for heating the dust to such temperatures include intense star formation, shocks, and the nuclear radiation.

In NGC 5252, a circumnuclear starburst can be ruled out (cf. § 1). In addition, the colors of the galaxy in the circumnuclear region are compatible with those of a passively evolved elliptical galaxy with moderate extinction (Kotilainen & Prieto 1995).

Heating by the nuclear radiation is not trivial if thermal equilibrium between dust grains and the nuclear radiation has to prevail. The nuclear luminosity of NGC 5252 is estimated as $L_f \sim (0.8\text{--}6.7) \times 10^{10} L_{\odot}$ (Kotilainen & Prieto 1995); the range reflects the variation in power-law spectral index; f is the covering factor. For $T = 175$ K, the dust should be placed at a maximum distance from the nucleus of $R = 12\text{--}30$ pc. This is a factor of 50–20 below the size of the emission at $15 \mu\text{m}$, ~ 650 pc radius. The nuclear luminosity may be greatly underestimated if the covering factor of the ionized gas is much lower than unity. Still, to increase R by a factor of 10, the luminosity should increase by a factor of 100. However, most important is the fact that the presumed thermal equilibrium cannot be applied to very small grains and PAHs, which are transiently heated to high temperatures by a single photon absorption, later reemitting their energy in the mid-IR. It is worth mentioning that the extended mid-IR emission in NGC 1068 does not present a radial variation of the color temperature as expected for a uniform distribution of dust grains (Bock et al. 2000). That could be explained in terms of very small grains transiently heated by the nuclear radiation field. The presence of PAHs in NGC 5252 cannot be confirmed from the present data. PAH emission is however claimed to be a general feature in the spectra of Seyfert 2 galaxies (Clavel et al. 2000), yet this emission is most probably linked to circumnuclear star-forming regions. Interestingly, to account for the near-IR emission in NGC 1068, Efstathiou, Hough, & Young (1995)

propose the existence of optically thin dust distributed within the ionization cone. The extended mid-IR emission in NGC 5252 may have similar origin.

Dust could also be heated by shocks, associated with, e.g., the propagation of the radio jet. The modeling of the nuclear SED and line spectrum requires shock excitation coupled with photoionization to provide a self-consistent account of the X-ray to radio properties of this galaxy (Contini, Prieto, & Viegas 1998). Shocks however do not appear to play a key role in the extended emission-line spectrum of the galaxy, which Contini et al. found to be dominated by the nuclear radiation only. Therefore, it seems improbable that the extended mid-IR emission be due to shock-heated dust.

An alternative possibility for the origin of the extended mid-IR is bremsstrahlung emission due to the mandatory cooling process of the photoionized and shock-heated gas. The bremsstrahlung component peaks in the optical–UV range, but its slowly decreasing tail, particularly in the near to mid-IR range, can greatly dominate the nuclear SED at these wavelengths (see Contini & Viegas 2000 for a thorough discussion). Thus, the extended near- to mid-IR emission in NGC 5252, and also perhaps in NGC 1068, may be associated with bremsstrahlung from the nuclear and extended ionized gas in the bicone.

4.2. The Nuclear IR Emission

Based on the arguments provided in § 3.2, the IR SED of NGC 5252 was separated into two main components: a nuclear component and a cold component ($T \sim 20$ K) associated with the galaxy as a whole. Because of the good definition of the 20 K galaxy component, the nuclear contribution can be isolated by subtracting that galaxy component from the total emission. The inferred IR luminosity for the residual component is 5.3×10^{43} ergs s⁻¹ (see Table 2). Kotilainen & Prieto (1995) provided an estimate for the hidden, nuclear optical/UV luminosity expected to be reprocessed by circumnuclear dust to be $L_{\text{repr}} \sim (2.6\text{--}8.5) \times 10^{43}$ ergs s⁻¹ (range varies depending on the assumed power-law spectral index of the ionizing radiation). Despite the uncertainties, both independently derived luminosities are in fair agreement and thus consistent with reprocessing of the nuclear radiation by circumnuclear dust.

The estimated mass of dust from the residual component is $\sim 10^5 M_{\odot}$ (Table 2). An alternative estimate of the mass of dust in the nucleus can be derived from extinction measurements. Kotilainen & Prieto (1995) found that the stellar galactic (in a $6''\text{--}12''$ ring) and nuclear (within a $3''$ region) light suffer an extinction of $A_V \sim 0.5$ mag and $A_V \sim 1$ mag, respectively. Assuming a canonical dust-to-gas mass ratio, those values imply dust masses of 6.7×10^5 and $1.2 \times 10^5 M_{\odot}$, respectively, in good agreement with the value for the nuclear component derived here (Table 2).

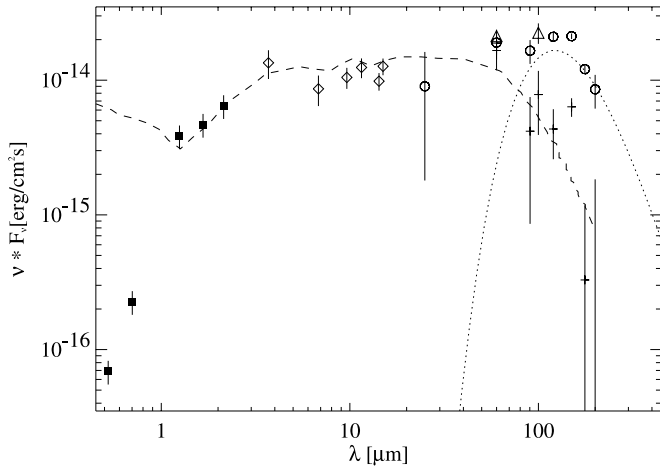


FIG. 3.—Residual SED after removing the galaxy component. Symbols are as in Fig. 2. Simple crosses represent the far-IR data after subtracting the 20 K component. The model proposed by Granato & Danese (1994) for NGC 1068 is shown as a dashed line. Note the large width of the IR bump, about two decades in wavelength.

The residual SED after removal of the galaxy component is shown in Figure 3. The first thing to notice is the width of the nuclear IR bump, which covers about two decades in wavelength. This “nuclear” SED is compared with current torus models next. The best compromise was found with Granato & Danese (1994) models. These are flared disk configurations characterized by a large radial extension, up to hundreds of parsecs, and a moderate optical thickness. Other models, such as the compact torus proposed by Pier & Krolik (1993) or the tapered disks by Efstathiou et al. (1995), would need additional components to account for the width of the bump and the near-IR part of the SED. Figure 3 shows the proposed model for NGC 1068 by Granato & Danese (1994) on top of the NGC 5252 nuclear SED. The overall match is remarkable and indicates that models supporting large disk structures should be further explored.

4.3. Very Cold Dust Emission

The IR luminosity and dust mass associated with the $T \simeq 20$ K component are given in Table 2. This component dominates the dust mass content of the galaxy. It is therefore worth comparing it with alternative galaxy mass estimates and with those derived from other galaxies of similar morphological type.

The dust mass derived from extinction measurements in the circumnuclear region of NGC 5252 (§ 4.2) is about a factor 100 below that inferred from the galaxy component (Table 2). Therefore, there is more dust in NGC 5252 apart from that detected in the circumnuclear region. Prieto & Freudling (1996) found H I emission distributed outside the ionization cones and extending about $1'$. A total mass of neutral gas of $1.8 \times 10^9 M_\odot$ is derived (an upper limit for the molecular gas of $3.6 \times 10^8 M_\odot$ is derived from millimetric observations). If the H I mass is compared with that derived

from the 20 K component, a gas-to-dust ratio of ~ 98 is found, very close to the canonical value. This suggests that the cold dust is probably related to the neutral gas and most probably spread throughout the galaxy.

It has been known since *IRAS* that early-type galaxies are not entirely devoid of interstellar material (Young et al. 1989), and NGC 5252 is not an exception. Bregman et al. (1998) studied the *IRAS* 60 and $100 \mu\text{m}$ emission of a sample of normal elliptical and S0 galaxies and interpreted the emission as due to dust being extended throughout the galaxy and, therefore, difficult to detect as obscuration patches. Their derived dust temperatures are likely overestimated since $100 \mu\text{m}$ is not yet on the falling turnover of the SED; hence, the dust masses are expected to be underestimated. For comparative purposes, the temperature and mass of the dust in NGC 5252 using the *IRAS* 60 and $100 \mu\text{m}$ fluxes only were derived. These yield $T_{\text{dust}} \sim 40$ K and $M \sim 1.4 \times 10^6 M_\odot$, respectively. Both values are well within the range found in Bregman’s sample but close to the highest ones, which may be a result of the fact that NGC 5252 harbors an active nucleus.

5. CONCLUSIONS

Based on new mid- and far-IR data collected with ISOCAM and ISOPHOT instruments, a detailed IR SED of the Seyfert 2 prototype NGC 5252 is presented. The main results are as follows.

1. The IR SED of NGC 5252 can be disentangled into two main components: a nuclear component accounting for the bulk of the luminosity in the $1\text{--}60 \mu\text{m}$ range and a cold component ($T \simeq 20$ K), peaking at about $100 \mu\text{m}$, associated with the galaxy as a whole. The latter accounts for 25% of the total IR luminosity and almost the totality of the dust mass content of the galaxy.

2. The mid-IR emission ($6\text{--}15 \mu\text{m}$) detected in ISOCAM images is concentrated toward the nuclear region of the galaxy. This emission is however resolved in all ISOCAM filters, but its morphology is undefined. A limit for the size of the region is set to $3''3$, ~ 1.3 kpc diameter. This size is consistent with that of the nucleus-obscuring structure seen in optical and near-IR color maps of the galaxy. Possible origins for this extended emission include small dust grains transiently heated by the nuclear radiation or bremsstrahlung from nuclear and extended ionized gas.

3. Comparison of the SED with current torus models favors models supporting large-scale disk structures. Indeed, the size of NGC 5252’s central obscuring structure and of the mid-IR region point to a kiloparsec-scale central disk.

The *COBE* data set was developed by the NASA Goddard Space Flight Center under the guidance of the *COBE* Science Working Group and was provided by the NSSDC. Ana Pérez García provided us with the results from the SED inversion method.

REFERENCES

- Abraham, P. A., Acosta-Pulido, J. A., Klaas, U., Bianchi, S., Radovich, M., & Schmidtobreik, L. 2003, in *The Calibration Legacy of the ISO Mission* (ESA-SP; Noordwijk: ESA), in press
- Acosta-Pulido, J. A., González-Hernández, J. I., Pérez García, A. M., & Rodríguez-Espinosa, J. M. 2001, in *ASP Conf. Ser. 249, The Central Kiloparsec of Active Galaxies and Starbursts*, ed. J. H. Knapen (San Francisco: ASP), 302
- Acosta-Pulido, J. A., Vila-Vilaró, B., Pérez-Fournon, I., Wilson, A. S., & Tsvetanov, Z. I. 1996, *ApJ*, 464, 177
- Bock, J. J., et al. 2000, *AJ*, 120, 2904
- Bregman, J. N., et al. 1998, *ApJ*, 499, 670
- Cameron, M., Storey, J. W. V., Rotaciuc, V., Genzel, R., Verstraete, L., Drapatz, S., Siebenmorgen, R., & Lee, T. J. 1993, *ApJ*, 419, 136
- Cappi, M., Mihara, T., Matsuoka, M., Brinkmann, W., Prieto, M. A., & Palumbo, G. G. C. 1996, *ApJ*, 456, 141
- Cesarsky, C. J., et al. 1996, *A&A*, 315, L32
- Clavel, J., et al. 2000, *A&A*, 357, 839
- Contini, M., Prieto, M. A., & Viegas, S. M. 1998, *ApJ*, 492, 511
- Contini, M., & Viegas, S. M. 2000, *ApJ*, 535, 721
- Danese, L., Zitelli, V., Granato, G., Wade, R., De Zotti, G., & Mandolesi, N. 1992, *ApJ*, 399, 38
- Edelson, R. A., Malkan, M. A., & Rieke, G. H. 1987, *ApJ*, 321, 233
- Efstathiou, R., Hough, J. H., & Young, S. 1995, *MNRAS*, 277, 1134
- Fouks, B. I., & Schubert, J. 1995, *Proc. SPIE*, 2475, 487
- Gabriel, C., Acosta-Pulido, J. A., Heinrichsen, I., Morris, H., Skaley, D., & Tai, W.-M. 1997, in *ASP Conf. Ser. 125, Astronomical Data Analysis Software and Systems VI*, ed. G. Hunt & H. E. Payne (San Francisco: ASP), 108
- Goodrich, R. W., Veilleux, S., & Hill, G. J. 1994, *ApJ*, 422, 521
- Granato, G. L., & Danese, L. 1994, *MNRAS*, 268, 235
- Kennicutt, R. C. 1998, *ARA&A*, 36, 189
- Kotilainen, J., & Prieto, M. A. 1995, *A&A*, 295, 646
- Krabbe, A., Böker, T., & Maiolino, R. 2001, *ApJ*, 557, 626
- Lemke, D., et al. 1996, *A&A*, 315, L64
- Osterbrock, D. E., & Martel, A. 1993, *ApJ*, 414, 552
- Ott, S., et al. 1997, in *ASP Conf. Ser. 125, Astronomical Data Analysis Software and Systems VI*, ed. G. Hunt & H. E. Payne (San Francisco: ASP), 34
- Pérez García, A. M., & Rodríguez Espinosa, J. M. 2001, *ApJ*, 557, 39
- Pérez García, A. M., Rodríguez Espinosa, J. M., & Santolaya Rey, A. E. 1998, *ApJ*, 500, 685
- Pier, E. A., & Krolik, J. 1993, *ApJ*, 418, 673
- Prieto, M. A., & Freudling, W. 1993, *ApJ*, 418, 668
- . 1996, *MNRAS*, 279, 63
- Prieto, M. A., Pérez García, A. M., & Rodríguez Espinosa, J. M. 2001, *A&A*, 377, 60
- . 2002, *MNRAS*, 329, 309
- Ruiz, M., Rieke, G. H., & Schmidt, G. D. 1994, *ApJ*, 423, 608
- Tadhunter, C., & Tsvetanov, Z. I. 1989, *Nature*, 341, 422
- Tsvetanov, Z. I., Morse, J. A., & Cecil, G. 1996, *ApJ*, 458, 172
- Young, J. S., Xie, S., Kenney, J. P. D., & Rice, W. L. 1989, *ApJS*, 70, 699